JACS
JOURNAL OF THE AMERICAN CHEMICAL SOCIETY
Article
pubs.acs.org/JACS

Computational Exploration of Rh^{III}/Rh^{V} and Rh^{III}/Rh^{I} Catalysis in Rhodium(III)-Catalyzed C−H Activation Reactions of *N*-Phenoxyacetamides with Alkynes

Yun-Fang Yang,[†,‡] K. N. Houk,[*,‡] and Yun-Dong Wu[*,†,§]

[†]Lab of Computational Chemistry and Drug Design, Laboratory of Chemical Genomics, Peking University Shenzhen Graduate School, Shenzhen 518055, China

[‡]Department of Chemistry and Biochemistry, University of California, Los Angeles, California 90095, United States

[§]College of Chemistry and Molecular Engineering, Peking University, Beijing 100871, China

Supporting Information

ABSTRACT: The selective rhodium-catalyzed functionalization of arenes is greatly facilitated by oxidizing directing groups that act both as directing groups and internal oxidants. We report density functional theory (B3LYP and M06) investigations on the mechanism of rhodium(III)-catalyzed redox coupling reaction of *N*-phenoxyacetamides with alkynes. The results elucidated the role of the internal oxidizing directing group, and the role of Rh^{III}/Rh^{I} and Rh^{III}/Rh^{V} catalysis of C−H functionalizations. A novel $Rh^{III}-Rh^{V}-Rh^{III}$ cycle successfully rationalizes recent experimental observations by Liu and Lu et al. (Liu, G. *Angew. Chem. Int. Ed.* **2013**, *52*, 6033) on the reactions of *N*-phenoxyacetamides with alkynes in different solvents. Natural Bond Orbital (NBO) analysis confirms the identity of Rh^{V} intermediate in the catalytic cycle.

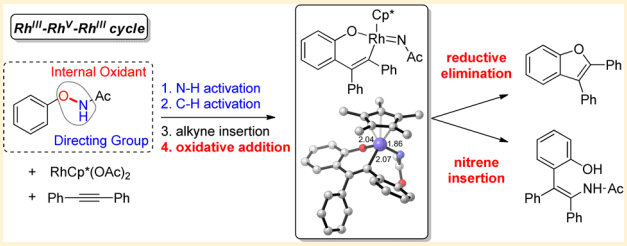

INTRODUCTION

Atom-economical synthesis is one of the top challenges in green chemistry.[1] The transition-metal-catalyzed oxidative coupling of arene C−H bonds with olefins, alkynes, or aldehydes is an attractive strategy that circumvents the need for prefunctionalization of the substrate.[2] However, such transformations generally require external oxidants like copper or silver salts to regenerate the catalyst and complete the catalytic cycle. As a consequence of the harsh oxidative conditions, substrate scope is limited, and the external oxidant residue is generated as waste. To avoid these drawbacks, the redox-neutral coupling reactions using internal oxidizing directing groups have been developed and have received much attention in recent years.[3]

The *N*-oxide, *N*-acyloxy, and *N*-methoxy, hydrazine, and nitroso groups are useful oxidizing directing groups.[4] Liu and Lu et al. reported rhodium(III)-catalyzed C−H functionalizations of the aryl group of *N*-phenoxyacetamides with alkynes. A subtle change in the reaction conditions can cause the reaction to produce either *ortho*-hydroxyphenyl-substituted enamides or benzofurans with high chemoselectivity (Scheme 1).[5] Methanol solvent favors the formation of the enamide product **P1**, while other solvents such as *t*BuOH, CH_2Cl_2, and toluene give the benzofuran **P2** as the major product.

However, the mechanisms of these transformations and how the pathways are altered by solvent are still unclear. We address through computations: (1) What are the detailed mechanisms of these reactions? (2) How do the solvents (MeOH vs CH_2Cl_2) alter the reaction pathway in redox-neutral coupling of *N*-phenoxyacetamides and alkynes? (3) How does the O−N bond act the role of internal oxidant to regenerate the catalyst?

Scheme 1. Rhodium(III)-Catalyzed C−H Functionalization of *N*-Phenoxyacetamides with Alkynes

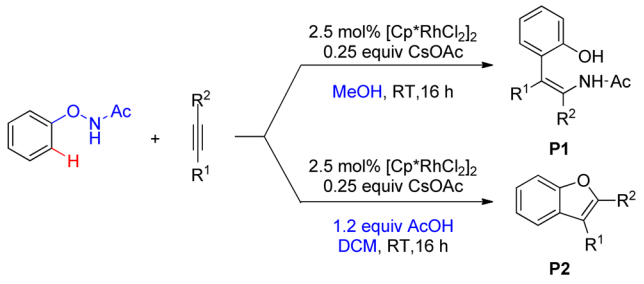

The $Rh^{III}-Rh^{I}-Rh^{III}$ catalytic cycle, shown in the top half of Scheme 2, is generally proposed for rhodium(III)-catalyzed, oxidizing directing groups-directed C−H activation and functionalization.[4,5] The first key step is C−H activation step that affords a five-membered rhodacycle intermediate **A**. The subsequent alkyne insertion step generates a seven-membered rhodacycle intermediate **B**. Reductive elimination of intermediate **B** gives Rh^{I} intermediate **C**, and this is followed by an oxidative addition step which breaks the O−N bond and forms

Received: April 3, 2016
Published: May 13, 2016

DOI: 10.1021/jacs.6b03424
J. Am. Chem. Soc. 2016, 138, 6861−6868

Scheme 2. Catalytic Cycle of Rhodium(III)-Catalyzed, Oxidizing Directing Groups-Directed C−H Activation and Functionalization

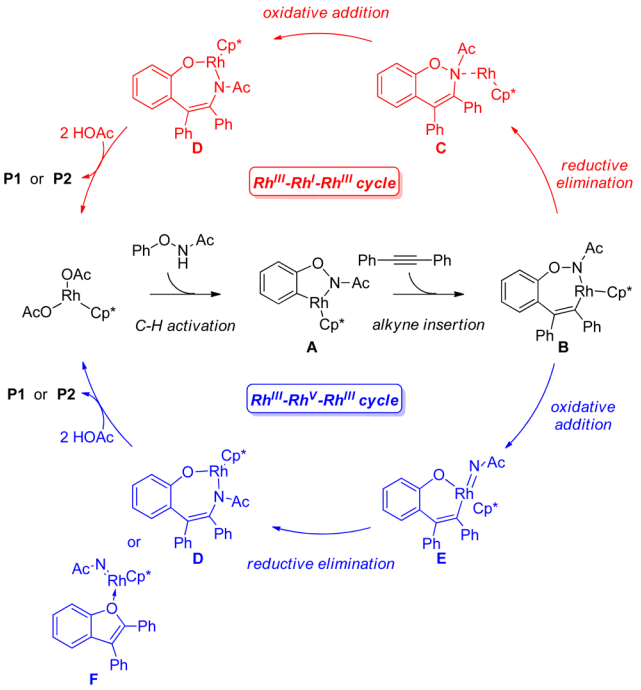

an isomeric seven-membered rhodacycle intermediate **D**. Finally, ligand exchange with acetic acid will generate the product and regenerate the Rh^{III} catalyst. An alternative catalytic cycle is the Rh^{III}−Rh^{V}−Rh^{III} cycle involving Rh^{V} species.[6] From **B**, the oxidative addition to the O−N bond occurs instead of the reductive elimination and the Rh^{V} species **E** is formed. The intermediate **E** can either undergo C−N reductive elimination to form **D**, or C−O reductive elimination to form **F**. Compared to the widely investigated Pd^{II}/Pd^{0} and Pd^{II}/Pd^{IV} catalysis,[7] Rh^{III}/Rh^{I} and Rh^{III}/Rh^{V} catalyses are less explored,[3−5] especially from a theoretical viewpoint. Therefore, we investigated both catalytic cycles to understand how the novel oxidizing directing groups play their roles.

Our study shows that the generally accepted mechanism in the reaction with *N*-phenoxyacetamide, the Rh^{I}−Rh^{III}−Rh^{I} catalytic cycle, requires a very high barrier of 32.0 kcal/mol. Instead, an unorthodox mechanism involving an Rh^{V}−nitrenoid intermediate is found favorable, with a barrier of only 24.6 kcal/mol. In the Rh^{III}−Rh^{V}−Rh^{III} catalytic cycle that we proposed, the N−O bond cleavage step is coupled with ring contraction, which allows a unique and facile pathway to achieve the Rh^{V}−nitrenoid intermediate. This adds an additional dimension to the current mechanistic picture, and will inspire not only the chemists that are interested in developing Rh-catalyzed C−H functionalization reactions with internal oxidant, but also the general audience that is interested in the generation and synthetic utility of Rh^{V}−nitrenoid species.

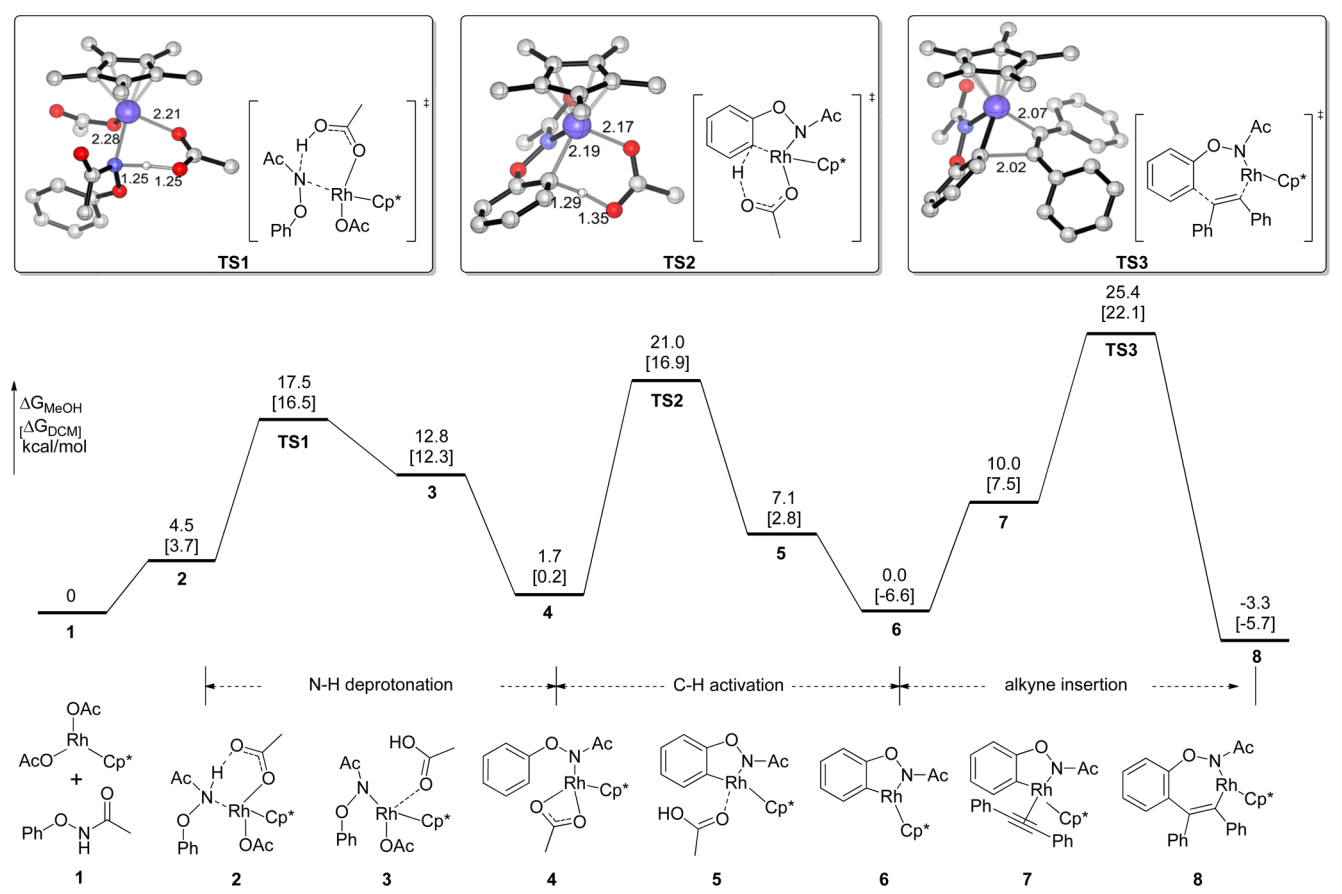

Figure 1. Free energy profiles in methanol [dichloromethane] for the initial three elementary steps of rhodium(III)-catalyzed redox-neutral coupling of *N*-phenoxyacetamide with diphenylacetylene, N−H activation, C−H activation, and alkyne insertion. The values (in kcal/mol) outside of the square brackets are computed with methanol solvent and those in the square brackets are computed with DCM solvent. For the CYLVIEW structures, hydrogen atoms except for the transferring proton are omitted for clarity.

DOI: 10.1021/jacs.6b03424
J. Am. Chem. Soc. 2016, 138, 6861−6868

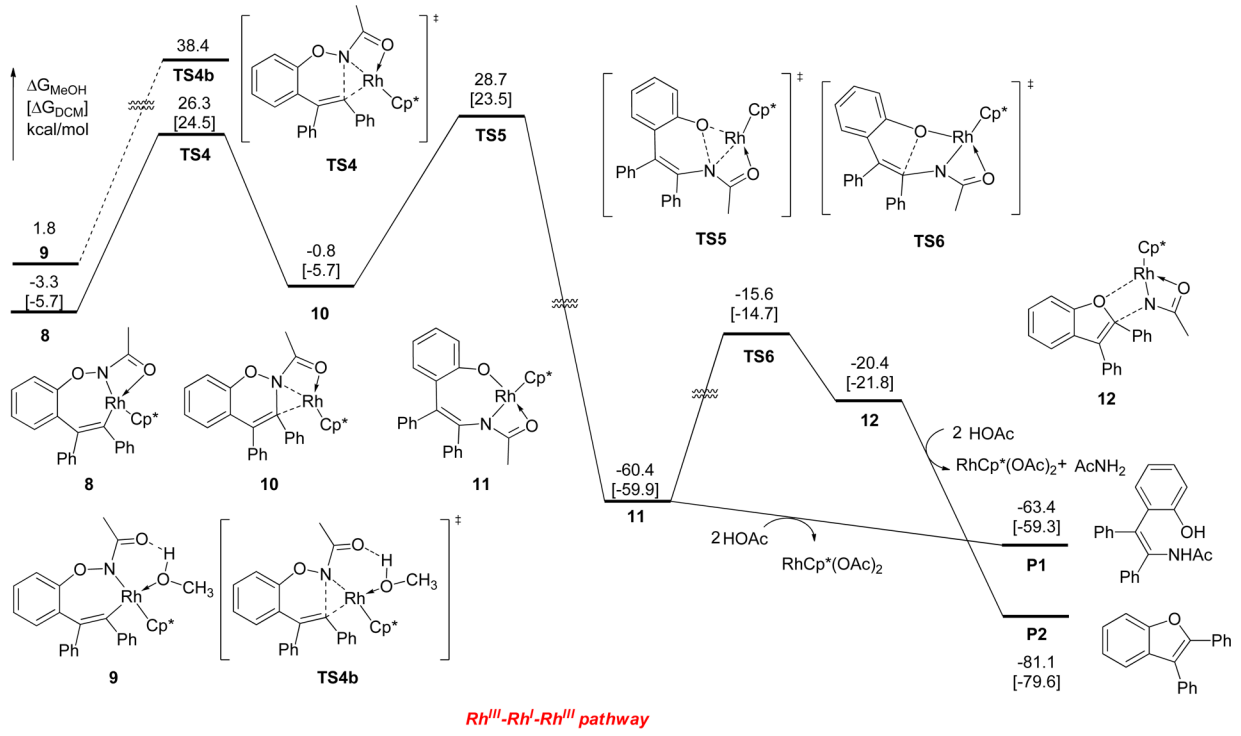

Figure 2. Free energy profiles in methanol [dichloromethane] for Rh^{III}–Rh^{I}–Rh^{III} catalytic mechanism of rhodium(III)-catalyzed redox-neutral coupling of *N*-phenoxyacetamide with diphenylacetylene.

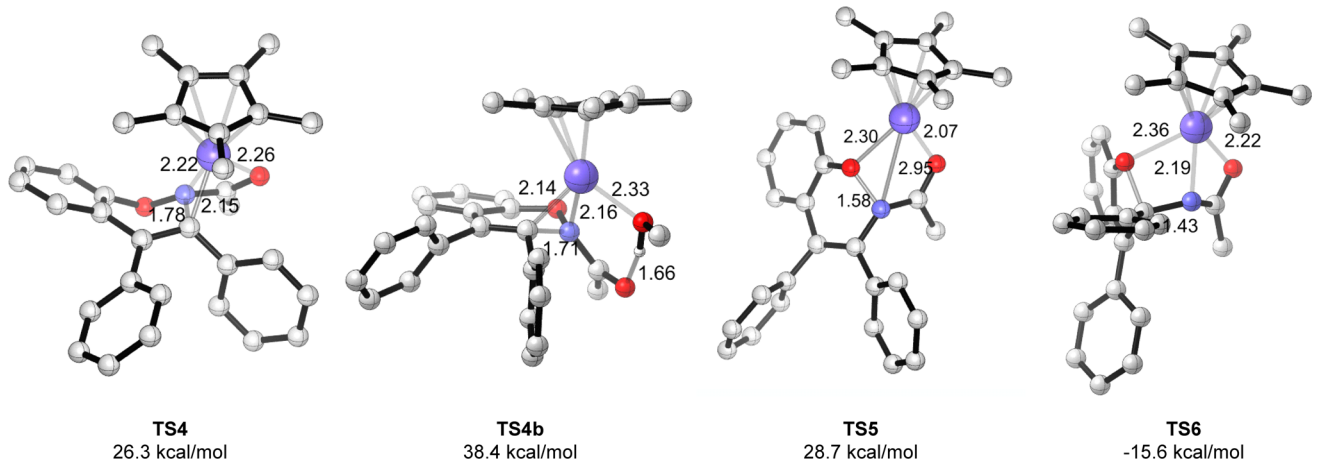

TS4 26.3 kcal/mol **TS4b** 38.4 kcal/mol **TS5** 28.7 kcal/mol **TS6** -15.6 kcal/mol

Figure 3. Optimized geometries of transition states **TS4**, **TS5** and **TS6**. Hydrogen atoms except the transferring proton are omitted for clarity.

COMPUTATIONAL DETAILS

All the calculations were carried out with the Gaussian 09 package.[8] Geometry optimization and energy calculations were performed with B3LYP.[9] The LANL2DZ basis set[10] with ECP was used for Rh, and the 6-31G (d) basis set[11] was used for other atoms. Frequency analysis was conducted at the same level of theory to verify the stationary points to be real minima or saddle points and to obtain the thermodynamic energy corrections. Single point energies were calculated at the M06[12]/ SDD[13]-6-311++G(d,p)[14] level using SMD[15] solvation model (solvent = methanol or dichloromethane). Computed structures are illustrated using CYLVIEW.[16]

RESULTS AND DISCUSSION

Rhodacycle Formation in Rhodium(III)-Catalyzed Redox-Neutral Coupling of *N*-Phenoxyacetamides and Alkynes. Figure 1 shows the computational results for the rhodium(III)-catalyzed redox-neutral coupling of *N*-phenoxyacetamide with diphenylacetylene that are common to all mechanisms. The transition structures are shown in the top of Figure 1. We computed steps for N–H deprotonation, C–H activation, and alkyne insertion. The consecutive N–H and C–H double activation has been widely investigated in transition-metal-catalyzed oxidative coupling.[17] Both of these steps are proposed to involve a concerted metalation–deprotonation (CMD) process,[18] with transition states **TS1** and **TS2**, respectively. The subsequent alkyne insertion transition state **TS3** (25.4 kcal/mol) has higher activation energy than both **TS1** (17.5 kcal/mol) and **TS2** (21.0 kcal/mol). The solvent models with both methanol and dichloromethane (DCM) were investigated, as shown in Figure 1. Most of the structures in methanol have higher energy than in DCM. The computational results suggest that C–H activation is not the rate-determining

DOI: 10.1021/jacs.6b03424
J. Am. Chem. Soc. 2016, 138, 6861–6868

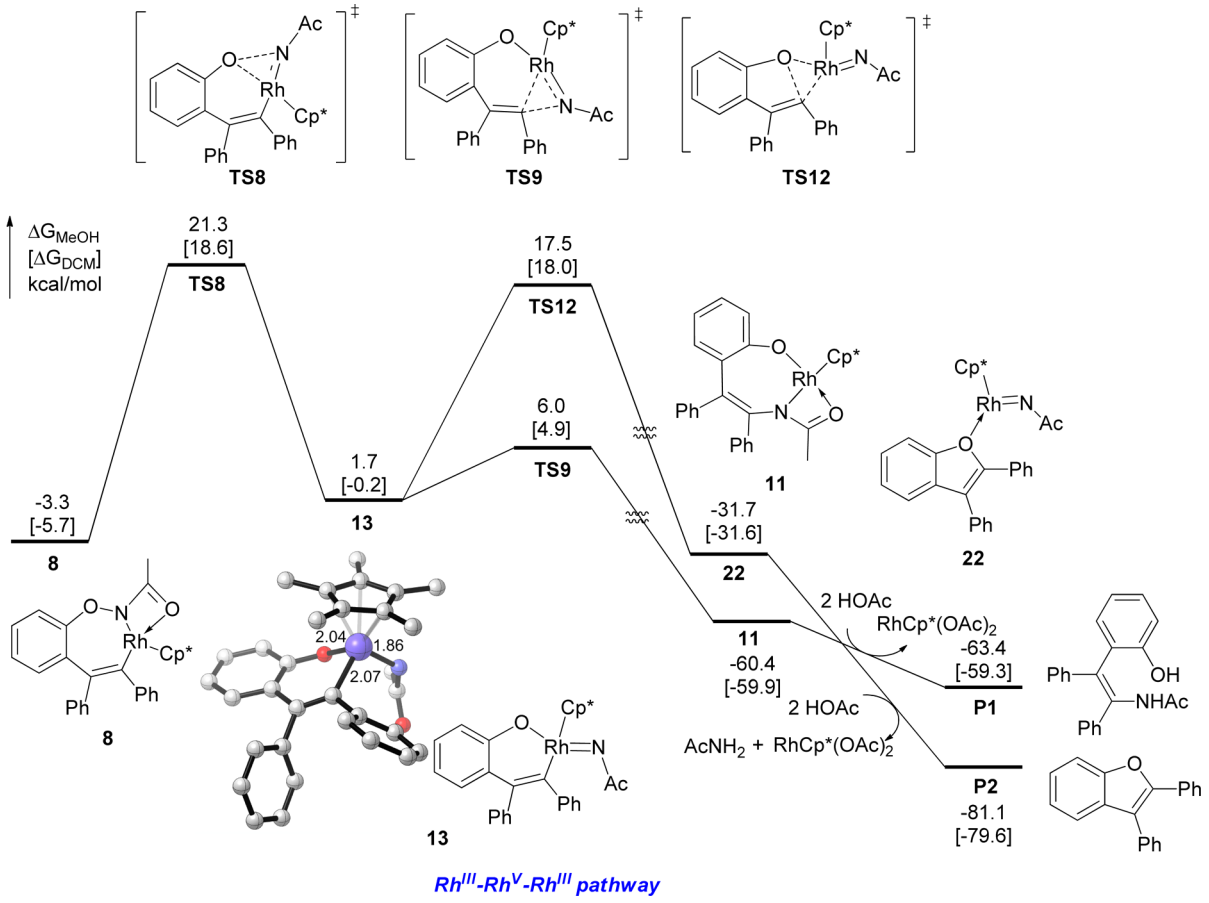

Figure 4. Free energy profiles in methanol [dichloromethane] for Rh^{III}–Rh^{V}–Rh^{III} catalytic mechanism of rhodium(III)-catalyzed redox-neutral coupling of *N*-phenoxyacetamide with diphenylacetylene.

step, and this is consistent with the small experimental KIE (k_H/k_D = 1.4–1.5).[5]

Rh^{III}–Rh^{I}–Rh^{III} Catalytic Mechanism for Rhodium(III)-Catalyzed Redox-Neutral Coupling of *N*-Phenoxyacetamides and Alkynes. The free energy profile of the Rh^{III}–Rh^{I}–Rh^{III} catalytic mechanism starting from rhodacycle intermediate **8** is shown in Figure 2. The formation of both *ortho*-hydroxyphenyl-substituted enamide product **P1** and the benzofuran product **P2** occur through the same initial steps, C–N reductive elimination and then N–O oxidation.[5] **TS4** and **TS5**, shown in Figure 3, are the transition states for these two steps, and have barriers of 29.6 and 32.0 kcal/mol as compared to intermediate **8**, respectively, with methanol solvent. These barriers are higher than that for the alkyne insertion step (25.4 kcal/mol for **TS3**). We have thoroughly studied the possibility of additional methanol coordination in all the intermediates and transition states. For example, in the key C–N bond formation step, the transition state with an additional methanol coordination, **TS4b**, is 12.1 kcal/mol higher in free energy as compared to that without the methanol coordination, **TS4** (Figure 2). We have found a similar situation exists for all the other species; either no coordination site is available in rhodium or the additional methanol coordination is unfavorable in free energy.

The C–N reductive elimination transition state **TS4** leads to structure **10**, in which the alkenyl ligand is weakly coordinate to the Rh center. Reorientation of the Rh center to the O–N bond can occur through transition state **TS5** to break the O–N bond and form intermediate **11**. From **11**, a facile protonation by acetic acid can occur to produce enamide product **P1**, or the alternative C–O bond formation/cyclization gives the benzofuran product **P2**. This C–O bond formation via **TS6** has a very high barrier of 44.8 kcal/mol. In the report by Liu and Lu et al., they proposed that the intermediate **8** can be protonated by HOAc to get a vinyl–Rh(III) intermediate, which can undergo intramolecular attack to give the cyclized benzofuran product. We cannot locate a concerted transition state for the proposed O–N bond cleavage and cyclization. A one-dimensional scan calculation for the C–O bond formation from the vinyl–Rh(III) type intermediate showed a barrier of 36 kcal/mol. We also investigated a stepwise mechanism for the O–N bond cleavage and cyclization from the vinyl–Rh(III) intermediate, and the transition state for O–N bond cleavage is 26.0 kcal/mol. This will lead to the formation of intermediate **24**, an Rh^{V} species, shown in Figure S1 (Supporting Informaiton). The subsequent elimination will give the benzofuran product **P2**. This stepwise pathway for the generation of benzofuran product requires a 29.3 kcal/mol overall barrier from intermediate **8**.

Rh^{III}–Rh^{V}–Rh^{III} Catalytic Mechanism for Rhodium(III)-Catalyzed Redox-Neutral Coupling of *N*-Phenoxyacetamides and Alkynes. In addition to the Rh^{III}–Rh^{I}–Rh^{III} catalytic mechanism, we studied a Rh^{III}–Rh^{V}–Rh^{III} catalytic mechanism with the oxidation of O–N bond to Rh^{III} occurring before the reductive elimination step (Figure 4). Interestingly, this new oxidative addition model **TS8** is accompanied by a ring contraction from 7-membered rhodacycle to 6-membered rhodacycle and leads to the formation of the Rh^{V} nitrenoid

DOI: 10.1021/jacs.6b03424
J. Am. Chem. Soc. 2016, 138, 6861–6868

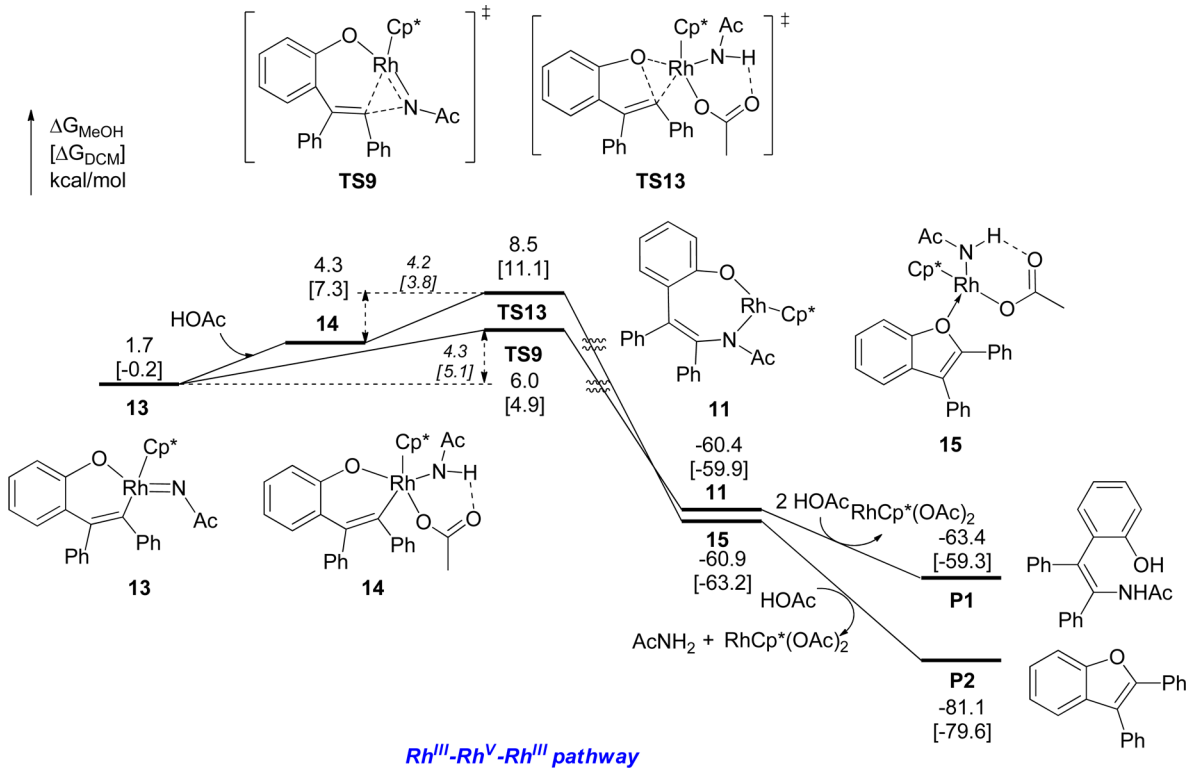

Figure 5. Free energy profiles in methanol [dichloromethane] for an alternative Rh^{III}–Rh^{V}–Rh^{III} catalytic mechanism of rhodium(III)-catalyzed redox-neutral coupling of *N*-phenoxyacetamide with diphenylacetylene.

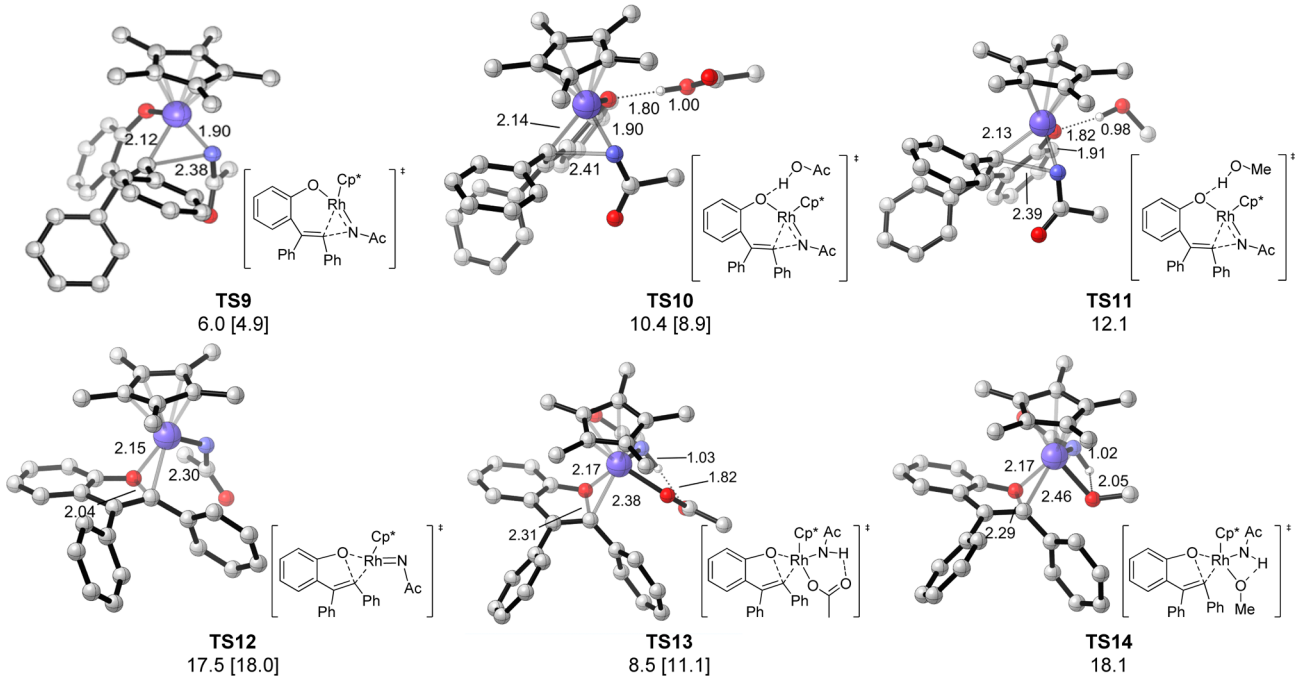

Figure 6. Optimized geometries and free energies for reductive elimination transition states. Hydrogen atoms are omitted for clarity.

species **13**. The barrier of cleavage of the O–N bond (via **TS8**) is 24.6 kcal/mol, lower than that of C–N reductive elimination (via **TS4**) by about 5 kcal/mol. The formation of Rh^{V} nitrenoid intermediate **13**, shown in Figure 4, is a very key process. In fact, there are examples of metal-mediated reactions involving Rh^{V} species.[6]

From the Rh^{V} nitrenoid intermediate **13**, a C–N reductive elimination (nitrene insertion) can occur to produce intermediate **11**, and subsequent protonation leads to product **P1**. The generation of **P1** through this pathway requires a 4.3 kcal/mol barrier via **TS9** as compared to the Rh^{V} nitrenoid intermediate **13**. We have also studied another possible pathway for the generation of **P1** via the protonation of **13**,

DOI: 10.1021/jacs.6b03424
J. Am. Chem. Soc. 2016, 138, 6861–6868

and found it unfavorable (Figure S2, Supporting Information). A C−O reductive elimination from **13** via transition state **TS12** leads to the formation of benzofuran product **P2**. The generation of **P2** through this pathway requires a 15.8 kcal/mol barrier as compared to the Rh^{V} nitrenoid intermediate **13**. It is very unfavorable as compared to the pathway for generation of **P1** via **TS9**.

Alternatively, an additional HOAc can coordinate to the Rh^{V} nitrenoid intermediate **13**, generating the intermediate **14** (Figure 5). This intermediate can then undergo a C−O reductive elimination via **TS13** to give the benzofuran coordinated complex **15**, and subsequent product liberation produces the benzofuran product **P2**.

The competition between **TS9** and **TS13** determines the chemoselectivity between **P1** and **P2**. These are very close in energy, and correct prediction of selectivities is very difficult because of inaccuracies in solvation models as well as problems in calculating entropies of the HOAc coordination step, from **13** to **14**. The problem of correctly calculate the entropies of bimolecular product in solution is well-known.[19] To understand the solvent effect on the product distribution, we compared the barriers between the transition state and its preceding intermediate. This alternative strategy avoids the HOAc coordination step and provides a meaningful way to study the solvent effect on the competing transition states. With methanol solvent (ε = 32.6), the barrier for C−O reductive elimination, **14** to **TS13**, is 4.2 kcal/mol, and the barrier for C−N reductive elimination, **13** to **TS9**, is 4.3 kcal/mol. With dichloromethane solvent (ε = 8.9), the barrier of C−O reductive elimination decreases to 3.8 kcal/mol, while the C−N reductive elimination barrier increases to 5.1 kcal/mol. These changes suggest that lowering the polarity of solvent disfavors the C−N reductive elimination step and the formation of enamide product **P1**. We also studied the possible methanol or acetic acid coordination on the C−N reductive elimination transition states that may affect the chemoselectivity, and found those postulated species all have higher free energies (Figure 6). Therefore, the solvent-controlled formation of **P1** or **P2** is most likely due to the polarity of methanol instead of its ligand role. Consistent with this postulate, the thorough experimental examination of solvents by Liu and Lu et al. also showed the trend that higher polarity solvents, such as MeOH and ethylene glycol, favor the formation of enamide product **P1**, while lower polarity solvents, such as *t*BuOH, *t*AmOH, CH_2Cl_2, and toluene, favor the formation of benzofuran product **P2**.

In addition to the solvent effect on the chemoselectivity, our computation also suggests that HOAc is important for the generation of benzofuran product **P2**, because an additional HOAc is involved in **TS13** to facilitate the C−O reductive elimination. For the ester-substituted alkyne, methyl 2-butynoate, the product ratio depends highly on the additive. With the general conditions, it is found that the benzofuran product is favored, while the addition of anion-exchange resin (Amberlite IRA-400) significantly changes the chemoselectivity and makes enamide the major product. Our calculations have shown that HOAc plays an important role in the formation of benzofuran product (Figure S3), and the C−O reductive elimination is greatly facilitated with an additional HOAc. This is consistent with the experimental observation that neutralizing the acetic acid disfavors the formation of the benzofuran.

Comparison between Rh^{III}−Rh^{I}-Rh^{III} and Rh^{III}−Rh^{V}-Rh^{III} Catalytic Mechanisms for Rhodium(III)-Catalyzed Redox-Neutral Coupling Reactions. To compare the Rh^{III}−Rh^{I}−Rh^{III} and Rh^{III}−Rh^{V}−Rh^{III} catalytic mechanisms for formation of **P2**, the key steps for the two mechanisms are shown in Figure 7. Common steps are shown in black, with Rh^{III}−Rh^{I}−Rh^{III} unique steps in red, and Rh^{III}−Rh^{V}−Rh^{III} unique steps in blue.

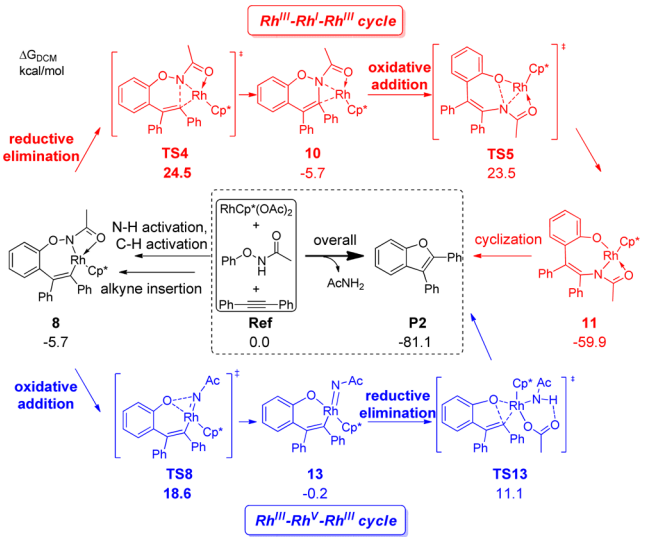

Figure 7. Comparison between Rh^{III}−Rh^{I}−Rh^{III} and Rh^{III}−Rh^{V}−Rh^{III} catalytic mechanism for rhodium(III)-catalyzed redox-neutral coupling of *N*-phenoxyacetamide and diphenylacetylene in dichloromethane.

The oxidative addition transition state **TS8** in Rh^{III}/Rh^{V} catalysis is about 6 kcal/mol lower than the reductive elimination transition state **TS4** in Rh^{III}/Rh^{I} catalysis in dichloromethane. The high barriers for direct reductive elimination for C−N bond formation are due to an unfavorable $C(sp^2)$−Rh−$N(sp^3)$ reductive elimination. It is interesting that the oxidation of O−N bond to Rh^{III} (**TS8**) is favorable in contrast to that to Rh^{I} (**TS5**).

To further evaluate the property of high-valent Rh^{V} nitrenoid species, we have performed the Natural Bond Orbital (NBO) analysis.[20] From intermediate **8** to **TS8**, and further to intermediate **13**, the Rh^{V}-species, NBO charge on the rhodium center changes from 0.217 to 0.256, and further to 0.387. This demonstrates that the electron density at the rhodium center is diminished. The electron binding energy obtained from NBO calculation is an index to evaluate the electronic contribution of the metal center during the oxidative/reductive process.[21] For metal centers with similar ligand environments, higher electron binding energies correlate with higher oxidation states of the metal center. For the oxidative addition of O−N bond to Rh^{III} center to form Rh^{V} species, the electron binding energy is expected to increase because the electron is less effectively shielded from the nuclear charge. The electron binding energy of the Rh 4s electron for intermediate **8**, **TS8**, and intermediate **13** is 85.8, 86.0, and 86.9 eV, respectively. This correlates well with the proposed change of oxidation state in the Rh center.

CONCLUSION

Density functional theory investigations have elucidated the mechanism of rhodium(III)-catalyzed C−H activation and functionalization with the oxidizing directing group O−N bond of *N*-phenoxyacetamide. We found that the oxidative addition of the covalent bond in oxidizing directing group occurs before reductive elimination. Therefore, the Rh^{III}−Rh^{V}−Rh^{III} mecha-

DOI: 10.1021/jacs.6b03424
J. Am. Chem. Soc. 2016, 138, 6861−6868

nism is much more favorable than the $Rh^{III}-Rh^{I}-Rh^{III}$ mechanism. Further NBO analysis supports the identity of Rh(V)−nitrenoid intermediate. These detailed computational studies provide further insight into the role of oxidizing directing groups in Rh (III)-catalyzed C−H activation reactions.

■ ASSOCIATED CONTENT

Supporting Information

The Supporting Information is available free of charge on the ACS Publications website at DOI: 10.1021/jacs.6b03424.

Additional mechanistic explorations and Cartesian coordinates of optimized structures (PDF)

■ AUTHOR INFORMATION

Corresponding Authors

*houk@chem.ucla.edu

*wuyd@pkusz.edu.cn

Notes

The authors declare no competing financial interest.

■ ACKNOWLEDGMENTS

We are grateful to the National Natural Science Foundation of China (21133002, 21203004), the Shenzhen Peacock Program (KQTD201103), the National Science Foundation of the USA (CHE-1361104), and the National Science Foundation under the CCI Center for Selective C−H Functionalization (CHE-1205646) for financial support of this research. Calculations were performed on the Hoffman2 cluster at UCLA and the Extreme Science and Engineering Discovery Environment (XSEDE), which is supported by the National Science Foundation (OCI-1053575).

■ REFERENCES

(1) (a) Anastas, P.; Eghbali, N. *Chem. Soc. Rev.* **2010**, *39*, 301. (b) Zhang, F.; Spring, D. R. *Chem. Soc. Rev.* **2014**, *43*, 6906. (c) Koschker, P.; Kähny, M.; Breit, B. *J. Am. Chem. Soc.* **2015**, *137*, 3131.

(2) (a) Colby, D. A.; Bergman, R. G.; Ellman, J. A. *Chem. Rev.* **2010**, *110*, 624. (b) Engle, K. M.; Mei, T.-S.; Wasa, M.; Yu, J.-Q. *Acc. Chem. Res.* **2012**, *45*, 788. (c) Li, Q.; Yu, Z.-X. *Angew. Chem., Int. Ed.* **2011**, *50*, 2144. (d) Musaev, D. G.; Kaledin, A.; Shi, B.-F.; Yu, J.-Q. *J. Am. Chem. Soc.* **2012**, *134*, 1690. (e) Zhang, Q.; Yu, H.-Z.; Li, Y.-T.; Liu, L.; Huang, Y.; Fu, Y. *Dalton Trans.* **2013**, *42*, 4175. (f) Qin, C.; Davies, H. M. L. *J. Am. Chem. Soc.* **2014**, *136*, 9792.

(3) (a) Patureau, F. W.; Glorius, F. *Angew. Chem., Int. Ed.* **2011**, *50*, 1977. (b) Chen, Y.; Wang, D.; Duan, P.; Ben, R.; Dai, L.; Shao, X.; Hong, M.; Zhao, J.; Huang, Y. *Nat. Commun.* **2014**, *5*, 4610. (c) Zhang, H.; Wang, K.; Wang, B.; Yi, H.; Hu, F.; Li, C.; Zhang, Y.; Wang, J. *Angew. Chem., Int. Ed.* **2014**, *53*, 13234. (d) Yu, S.; Liu, S.; Lan, Y.; Wan, B.; Li, X. *J. Am. Chem. Soc.* **2015**, *137*, 1623.

(4) (a) Wu, J.; Cui, X.; Chen, L.; Jiang, G.; Wu, Y. *J. Am. Chem. Soc.* **2009**, *131*, 13888. (b) Tan, Y.; Hartwig, J. F. *J. Am. Chem. Soc.* **2010**, *132*, 3676. (c) Ng, K.-H.; Chan, A. S. C.; Yu, W.-Y. *J. Am. Chem. Soc.* **2010**, *132*, 12862. (d) Guimond, N.; Gouliaras, C.; Fagnou, K. *J. Am. Chem. Soc.* **2010**, *132*, 6908. (e) Guimond, N.; Gorelsky, S. I.; Fagnou, K. *J. Am. Chem. Soc.* **2011**, *133*, 6449. (f) Rakshit, S.; Grohmann, C.; Besset, T.; Glorius, F. *J. Am. Chem. Soc.* **2011**, *133*, 2350. (g) Huckins, J. R.; Bercot, E. A.; Thiel, O. R.; Hwang, T.-L.; Bio, M. M. *J. Am. Chem. Soc.* **2013**, *135*, 14492. (h) Zhao, D.; Shi, Z.; Glorius, F. *Angew. Chem., Int. Ed.* **2013**, *52*, 12426. (i) Wang, C.; Huang, Y. *Org. Lett.* **2013**, *15*, 5294. (j) Liu, B.; Song, C.; Sun, C.; Zhou, S.; Zhu, J. *J. Am. Chem. Soc.* **2013**, *135*, 16625. (k) Huang, X.; Huang, J.; Du, C.; Zhang, X.; Song, F.; You, J. *Angew. Chem., Int. Ed.* **2013**, *52*, 12970. (l) Fukui, Y.; Liu, P.; Liu, Q.; He, Z.-T.; Wu, N.-Y.; Tian, P.; Lin, G.-Q. *J. Am. Chem. Soc.* **2014**, *136*, 15607. (m) Sharma, U.; Park, Y.; Chang, S. *J. Org. Chem.* **2014**, *79*, 9899. (n) Chen, W.-J.; Lin, Z. *Organometallics* **2015**, *34*, 309.

(5) Liu, G.; Shen, Y.; Zhou, Z.; Lu, X. *Angew. Chem., Int. Ed.* **2013**, *52*, 6033.

(6) (a) Chen, H.; Schlecht, S.; Semple, T. C.; Hartwig, J. F. *Science* **2000**, *287*, 1995. (b) Brayshaw, S. K.; Sceats, E. L.; Green, J. C.; Weller, A. S. *Proc. Natl. Acad. Sci. U. S. A.* **2007**, *104*, 6921. (c) Vyboishchikov, S. F.; Nikonov, G. I. *Organometallics* **2007**, *26*, 4160. (d) McBee, J. L.; Escalada, J.; Tilley, T. D. *J. Am. Chem. Soc.* **2009**, *131*, 12703. (e) Xu, L.; Zhu, Q.; Huang, G.; Cheng, B.; Xia, Y. *J. Org. Chem.* **2012**, *77*, 3017. (f) Wencel-Delord, J.; Nimphius, C.; Patureau, F. W.; Glorius, F. *Angew. Chem., Int. Ed.* **2012**, *51*, 2247. (g) Schröder, N.; Wencel-Delord, J.; Glorius, F. *J. Am. Chem. Soc.* **2012**, *134*, 8298. (h) Ryu, J.; Shin, K.; Park, S. H.; Kim, J. Y.; Chang, S. *Angew. Chem., Int. Ed.* **2012**, *51*, 9904. (i) Shin, K.; Baek, Y.; Chang, S. *Angew. Chem., Int. Ed.* **2013**, *52*, 8031. (j) Park, S. H.; Kwak, J.; Shin, K.; Ryu, J.; Park, Y.; Chang, S. *J. Am. Chem. Soc.* **2014**, *136*, 2492. (k) Shin, K.; Kim, H.; Chang, S. *Acc. Chem. Res.* **2015**, *48*, 1040. (l) Zhou, T.; Guo, W.; Xia, Y. *Chem. - Eur. J.* **2015**, *21*, 9209. (m) Li, J.; Qiu, Z. *J. Org. Chem.* **2015**, *80*, 10686.

(7) (a) Whitfield, S. R.; Sanford, M. S. *J. Am. Chem. Soc.* **2007**, *129*, 15142. (b) Chen, X.; Engle, K. M.; Wang, D.-H.; Yu, J.-Q. *Angew. Chem., Int. Ed.* **2009**, *48*, 5094. (c) Shabashov, D.; Daugulis, O. *J. Am. Chem. Soc.* **2010**, *132*, 3965. (d) Powers, D. C.; Ritter, T. *Acc. Chem. Res.* **2012**, *45*, 840. (e) Neufeldt, S. R.; Sanford, M. S. *Acc. Chem. Res.* **2012**, *45*, 936.

(8) Frisch, M. J.; Trucks, G. W.; Schlegel, H. B.; Scuseria, G. E.; Robb, M. A.; Cheeseman, J. R.; Scalmani, G.; Barone, V.; Mennucci, B.; Petersson, G. A.; Nakatsuji, H.; Caricato, M.; Li, X.; Hratchian, H. P.; Izmaylov, A. F.; Bloino, J.; Zheng, G.; Sonnenberg, J. L.; Hada, M.; Ehara, M.; Toyota, K.; Fukuda, R.; Hasegawa, J.; Ishida, M.; Nakajima, T.; Honda, Y.; Kitao, O.; Nakai, H.; Vreven, T.; Montgomery, J. A., Jr.; Peralta, J. E.; Ogliaro, F.; Bearpark, M.; Heyd, J. J.; Brothers, E.; Kudin, K. N.; Staroverov, V. N.; Keith, T.; Kobayashi, R.; Normand, J.; Raghavachari, K.; Rendell, A.; Burant, J. C.; Iyengar, S. S.; Tomasi, J.; Cossi, M.; Rega, N.; Millam, J. M.; Klene, M.; Knox, J. E.; Cross, J. B.; Bakken, V.; Adamo, C.; Jaramillo, J.; Gomperts, R.; Stratmann, R. E.; Yazyev, O.; Austin, A. J.; Cammi, R.; Pomelli, C.; Ochterski, J. W.; Martin, R. L.; Morokuma, K.; Zakrzewski, V. G.; Voth, G. A.; Salvador, P.; Dannenberg, J. J.; Dapprich, S.; Daniels, A. D.; Farkas, O.; Foresman, J. B.; Ortiz, J. V.; Cioslowski, J.; Fox, D. J. *Gaussian 09*, Rev. D.01; Gaussian, Inc.: Wallingford, CT, 2010.

(9) (a) Lee, C.; Yang, W.; Parr, R. G. *Phys. Rev. B: Condens. Matter Mater. Phys.* **1988**, *37*, 785. (b) Becke, A. D. *J. Chem. Phys.* **1993**, *98*, 1372. (c) Becke, A. D. *J. Chem. Phys.* **1993**, *98*, 5648. (d) Stephens, P. J.; Devlin, F. J.; Chabalowski, C. F.; Frisch, M. J. *J. Phys. Chem.* **1994**, *98*, 11623.

(10) (a) Hay, P. J.; Wadt, W. R. *J. Chem. Phys.* **1985**, *82*, 299. (b) Ehlers, A. W.; Böhme, M.; Dapprich, S.; Gobbi, A.; Höllwarth, A.; Jonas, V.; Köhler, K. F.; Stegmann, R.; Veldkamp, A.; Frenking, G. *Chem. Phys. Lett.* **1993**, *208*, 111. (c) Roy, L. E.; Hay, P. J.; Martin, R. L. *J. Chem. Theory Comput.* **2008**, *4*, 1029.

(11) (a) Ditchfield, R.; Hehre, W. J.; Pople, J. A. *J. Chem. Phys.* **1971**, *54*, 724. (b) Hehre, W. J.; Ditchfield, R.; Pople, J. A. *J. Chem. Phys.* **1971**, *54*, 2257. (c) Hariharan, P. C.; Pople, J. A. *Theor. Chim. Acta.* **1973**, *28*, 213.

(12) Zhao, Y.; Truhlar, D. G. *Theor. Chem. Acc.* **2008**, *120*, 215.

(13) (a) Dolg, M.; Wedig, U.; Stoll, H.; Preuss, H. *J. Chem. Phys.* **1987**, *86*, 866. (b) Andrae, D.; Häußermann, U.; Dolg, M.; Stoll, H.; Preuß, H. *Theor. Chem. Acc.* **1990**, *77*, 123.

(14) Krishnan, R.; Binkley, J. S.; Seeger, R.; Pople, J. A. *J. Chem. Phys.* **1980**, *72*, 650.

(15) Marenich, A. V.; Cramer, C. J.; Truhlar, D. G. *J. Phys. Chem. B* **2009**, *113*, 6378.

(16) Legault, C. Y. CYLView, 1.0b; Université de Sherbrooke, Canada, 2009; http://www.cylview.org.

DOI: 10.1021/jacs.6b03424
J. Am. Chem. Soc. 2016, 138, 6861−6868

(17) (a) Song, G.; Wang, F.; Li, X. *Chem. Soc. Rev.* **2012**, *41*, 3651. (b) Duan, P.; Yang, Y.; Ben, R.; Yan, Y.; Dai, L.; Hong, M.; Wu, Y.-D.; Wang, D.; Zhang, X.; Zhao, J. *Chem. Sci.* **2014**, *5*, 1574.
(18) (a) Winstein, S.; Traylor, T. G. *J. Am. Chem. Soc.* **1955**, *77*, 3747. (b) Lapointe, D.; Fagnou, K. *Chem. Lett.* **2010**, *39*, 1118. (c) Ackermann, L. *Chem. Rev.* **2011**, *111*, 1315. (d) Anand, M.; Sunoj, R. B. *Org. Lett.* **2011**, *13*, 4802. (e) Gong, T.-J.; Xiao, B.; Cheng, W.-M.; Su, W.; Xu, J.; Liu, Z.-J.; Liu, L.; Fu, Y. *J. Am. Chem. Soc.* **2013**, *135*, 10630. (f) O'Reilly, M. E.; Fu, R.; Nielsen, R. J.; Sabat, M.; Goddard, W. A.; Gunnoe, T. B. *J. Am. Chem. Soc.* **2014**, *136*, 14690. (g) Yang, Y.-F.; Cheng, G.-J.; Liu, P.; Leow, D.; Sun, T.-Y.; Chen, P.; Zhang, X.; Yu, J.-Q.; Wu, Y.-D.; Houk, K. N. *J. Am. Chem. Soc.* **2014**, *136*, 344. (h) Cheng, G.-J.; Yang, Y.-F.; Liu, P.; Chen, P.; Sun, T.-Y.; Li, G.; Zhang, X.; Houk, K. N.; Yu, J.-Q.; Wu, Y.-D. *J. Am. Chem. Soc.* **2014**, *136*, 894. (i) Sun, H.; Wang, C.; Yang, Y.-F.; Chen, P.; Wu, Y.-D.; Zhang, X.; Huang, Y. *J. Org. Chem.* **2014**, *79*, 11863. (j) Cheng, G.-J.; Zhang, X.; Chung, L. W.; Xu, L.; Wu, Y.-D. *J. Am. Chem. Soc.* **2015**, *137*, 1706.
(19) (a) Wertz, D. H. *J. Am. Chem. Soc.* **1980**, *102*, 5316. (b) Leung, B. O.; Reid, D. L.; Armstrong, D. A.; Rauk, A. *J. Phys. Chem. A* **2004**, *108*, 2720.
(20) (a) Reed, A. E.; Curtiss, L. A.; Weinhold, F. *Chem. Rev.* **1988**, *88*, 899. (b) Weinhold, F.; Landis, C. R. *Valency and Bonding: A Natural Bond Orbital Donor-Acceptor Perspective*; Cambridge University Press: Cambridge, U.K., 2005.
(21) Powers, D. C.; Benitez, D.; Tkatchouk, E.; Goddard, W. A.; Ritter, T. *J. Am. Chem. Soc.* **2010**, *132*, 14092.

DOI: 10.1021/jacs.6b03424
J. Am. Chem. Soc. 2016, 138, 6861−6868